Rotating Shocks in a Separated Laboratory Channel Flow*

L. J. PRATT†

Woods Hole Oceanographic Institution, Woods Hole, MA 02543

(Manuscript received 3 June 1986, in final form 17 October 1986)

ABSTRACT

Laboratory studies of the effects of wall separation on a hydraulic jump in a rotating channel of rectangular cross section are described. Separation is induced by increasing the rotation rate while maintaining a constant flow rate through the channel. It is found that separation can occur in the supercritical flow upstream of the jump but not in the subcritical downstream flow. At high rotation rates the 'jump' becomes one of stream width, rather than depth, and the associated turbulent eddies occur in the vertical plane rather than in the horizontal plane. Although depth changes occur across the jump, these changes are gradual and wavelike.

A simple shock-joining theory indicates that stationary shocks with separated upstream flow and attached downstream flow are possible within a certain range of upstream Froude and Burger numbers. This result supplements a theory due to Nof which indicates that stationary shocks are not possible when both upstream and downstream flows are separated.

1. Introduction

Interest has recently arisen concerning the possibility that hydraulic jumps, or some rotationally modified version thereof, might occur in the lees of certain deep overflows. For example, observations of the overflow in the Windward Passage show a region where the isothermal elevation increases abruptly in the downstream direction suggesting some sort of jump (Nof, 1986). From a fluid mechanical point of view the question is: Can some kind of stationary jump (or 'shock') exist in a strongly rotating overflow and, if so, what is its structure?

Yih et al. (1964), Houghton (1969) and Williams and Hori (1970) have studied the conditions under which rotating jumps form in solutions to the single-layer shallow water equations in a domain containing no side walls. Jump solutions exhibiting many of the qualitative features of nonrotating hydraulic jumps were found, however, the solutions are not directly relevant to oceanic overflows due to the neglect of lateral boundaries. More recently, Pratt (1983) and Nof (1986) found rotating jump solutions in channels of rectangular cross section. Pratt's solution was obtained numerically and an example is shown in Fig. 1. The jump occurs in the shallow supercritical flow slightly downstream of an obstacle and consists of an abrupt increase in free surface elevation. The jump amplitude decays away from the left wall (facing downstream) in the manner of a Kelvin wave. The decay scale (the Rossby radius of deformation) is here equal to the channel width. The solutions by Nof (1986) were obtained analytically under the assumptions: 1) that the jump in depth occurs on a line perpendicular to the channel axis, and 2) that the deformation radius is much greater than the channel width. The solution is similar to that of Fig. 1, except that the decay in the jump amplitude away from the left wall is small. In both cases, one expects to encounter intense turbulence and vertical mixing near the region of abrupt depth change (although this turbulence is not explicit in either calculation).

In both calculations described above, the fluid depth remains finite across the entire channel width. However, a close inspection of Fig. 1 reveals that the fluid depth at the left wall immediately upstream of the jump is nearly zero. In fact, a sufficient increase in the rotation rate would cause the fluid to separate from the left wall, leading to the formation of a free streamline at the left edge of the current and exposing a portion of the channel bottom. By further increasing the rotation rate, it presumably is possible to cause the stream to become separated along the entire length of channel. In this case, Kelvin wave propagation along the left edge of the stream is obviously impossible. Instead a wave whose properties are drastically different from those of the Kelvin wave arises (Stern, 1980; Kubokawa and Hanawa, 1984a,b). This wave is characterized by large lateral excursions of the free edge of the stream and, consequently, by large cross-channel velocities. (The cross-channel velocity in a Kelvin wave is zero.) One should therefore expect a dramatic change in the character of the jump to take place upon separation.

* Woods Hole Oceanographic Institution Contribution Number 6343.

† Temporary Address: Mail Code A-030, Scripps Institution of Oceanography, La Jolla, CA 92093.

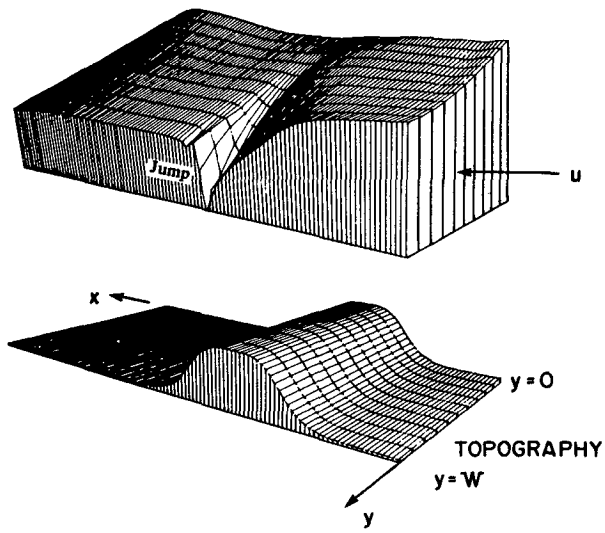

FIG. 1. Hydraulic jump in a rotating channel from numerical experiment of Pratt (1983). The flow is from right to left and the along-channel velocity u is geostrophic. Shown in the upper image are the free surface of the fluid and one of the walls of the rotating channel (the other wall and the topography are hidden). The lower image shows the bottom topography.

The implications of this problem are important, for the bottom flow in sea straits is often banked by rotation against one of the side walls, the left edge lying in a region of little or no cross-strait bottom slope. Unfortunately, the numerical method used by Pratt (1983) becomes unstable when separation occurs, and this interesting problem was not explored.

Also relevant to the problem of flow separation is a calculation by Nof (1984) showing the conditions under which shocks can form in a zero potential vorticity coastal (i.e., no 'left' wall) current. The shocks that are found are characterized by changes in the current depth *and* width. However, all such shocks are found to have a finite propagation speed; *no stationary shocks are possible.* The lack of a stationary shock can be motivated using a simple argument based on mass conservation: since the total mass flux in the coastal current is proportional to the square of the wall depth (see section 3), a stationary jump in depth cannot conserve mass.

What then happens to the jump in Fig. 1 if the rotation rate is increased? To investigate this intriguing question, a simple laboratory experiment was performed at the Woods Hole Oceanographic Institution's hydrodynamics laboratory. The experiments were carried out using a long tank of rectangular cross section (see Fig. 2) mounted on a turntable. A nonrotating planar hydraulic jump is first produced in the lee of the bottom-mounted obstacle by pumping fluid through the tank at a fixed flow rate. The tank is then rotated at various rates (with the flow rate kept constant) and the effects of rotation on the jump are observed, most notably that of separation.

There are several possible separation-induced changes in jump structure that are of interest. Provided that some coherent transition between the supercritical and subcritical flow persists, what is the orientation of the associated turbulent eddies relative to the nonrotating case? Second, is a 'free' jump in which both the subcritical and supercritical end states are separated possible for sufficiently large rotation rates? Finally, can a shock-joining theory be devised which describes the jumps that occur?

2. Apparatus and setup

Sketched in Fig. 2 is the design of the 250 cm long and 20 cm wide glass channel and recirculation system. After being fed into one end of the channel, water passes beneath a sluice gate, through a screen, and into a relatively deep reservoir located upstream of a large obstacle. By forcing the fluid through the screen slowly and at a uniform depth, one hopes to homogenize the vorticity and thus create a reservoir containing uniform potential vorticity fluid. From the reservoir, the water flows over the obstacle, becoming supercritical on its downstream face, and experiences a hydraulic jump. The position of the jump varies from 5 cm upstream to 5 cm downstream of the downstream edge of the obstacle and is controlled by adding or deleting water from the system. An increase in system volume causes the jump to move closer to the sill and the jump amplitude to decrease. For cases in which the jump lies downstream of the obstacle a slight (<4°) tilt is given to the tank for the purpose of stabilizing the position of the jump. At the left end of the tank far downstream from the jump, water is withdrawn uniformly across the width of the tank. The water is then fed through a flow meter and recirculated by means of a 2.5 hp, 500

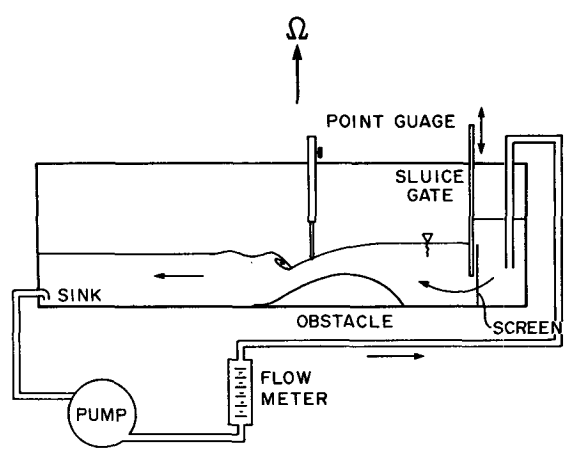

LABORATORY FLUME FOR STUDYING ROTATING JUMPS

FIG. 2. Design of rotating channel and recirculation system.

ml s^{-1} pump. As in other hydraulics experiments, some forcing mechanism is required downstream of the obstacle to produce a jump. The forcing may be due to a second obstacle or bottom friction; here it is due to the end wall. The means of fluid introduction and withdrawal, the tank tilt, and the position of the obstacle relative to the back wall are occasionally varied to insure that these conditions are not influencing the interior flow.

Once a jump is established, the system is spun up to a fixed angular speed, $f/2$ using the Woods Hole 2 meter diameter turntable. Rotation rates of up to $f = 2.5$ sec^{-1} were used. A more detailed description of this turntable is given by Whitehead (1985). Measurements of rotation-induced deformations of the free surface are made using a point gauge, and streamline patterns and approximate surface velocities are obtained using time-lapse photographs of surface floats. In the description of these observations, the coordinate system shown in Fig. 3 will be referred to, with x and y denoting the downstream and cross-stream directions. The walls at $y = W$ and $y = 0$ will be called the left and right walls, respectively, as an observer facing downstream would see. Also the terms 'jump' and 'shock' will be used interchangeably to describe any abrupt transition in fluid depth, velocity, etc. occurring in the downstream direction.

3. Scale analysis

The qualitative features of the classical planar hydraulic jump depend upon gravity g and the depth and velocity scales H_1 and U_1 of the flow immediately upstream of the jump. The only dimensionless number which can be formed from these scales is the Froude number:

$$F_1 = U_1/(gH)^{1/2} \tag{3.1}$$

and many of the gross features of the jump can be related to F_1, as discussed by Chow (1959, p. 395). For $1.0 < F_1 < 1.7$, the free surface within the jump is undular and smooth and the change in depth occurs over a distance that is large compared to the fluid depth.

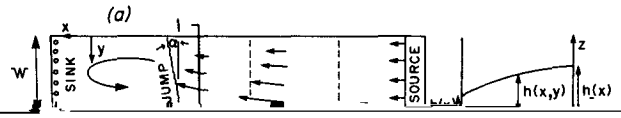

The present experiment concentrates on the case $F_1 > 1.7$ for which the nonrotating jump is a true 'shock', i.e., the depth change occurs over a distance comparable to the depth of the subcritical flow.

Rotation leads to the addition of a time scale f^{-1} and (at least) one lateral length scale. The latter is chosen as the stream width w_1, which may or may not be equal to the channel width W. In summary, there are now at least five dimensional quantities which characterize the approaching flow: $\bar{U}_1, \bar{H}_1, g, f$ and w_1. The subscript 1 denotes values taken immediately upstream of the jump, and the overbar indicates a typical value over a given cross-section. From these, it is possible to form three independent dimensionless numbers of which one, $\bar{H}_1/w_1$, remains small (<0.15) in all experiments. The other two are a generalized Froude number:

$$\bar{F}_1 = \bar{U}_1/(g\bar{H}_1)^{1/2} \tag{3.2}$$

and a Burger number:

$$r_1 = w_1 f/(g\bar{H}_1)^{1/2}. \tag{3.3}$$

If the along-channel velocity is approximately geostrophic at section 1, $u_1 = -gf^{-1}\partial h_1/\partial y$, then the flow rate $Q = \int_0^{w_1} uhdy$ can be expressed as

$$Q = gf^{-1}(h_{1-} - h_{1+})(h_{1-} + h_{1+})/2 \tag{3.4}$$

where h_{1+} and h_{1-} are the depths on the left and right edges of the current (facing downstream). Since Q should scale with $\bar{U}_1\bar{H}_1 w_1$, it is natural to set

$$\bar{H}_1 = (h_{1-} + h_{1+})/2 \tag{3.5}$$

$$\bar{U}_1 = g(fw_1)^{-1}(h_{1-} - h_{1+}). \tag{3.6}$$

If Q, f, g and h_{1-} are known, then h_{1+} can be computed from (3.4). The parameters $\bar{F}_1$ and r_1 can therefore be computed by measuring the single flow variable, h_{1-}.

If the flow is separated before the jump, $h_{1+} = 0$ and h_{1-} is given directly by (3.4). Furthermore, the geostrophic relation suggests that $\bar{U}_1$ should scale with gh_{1-}/fw_1 $(=2g\bar{H}_1/fw_1)$, implying

$$\bar{F}_1 r_1 = 2 \quad \text{(separated)}. \tag{3.7}$$

A 'free' jump (for which both end states are separated) would then be described by a single parameter, $\bar{F}_1$ or r_1. To compute either, it is necessary only to measure Q, f and w_1. Another possibility is that the flow is separated upstream but not downstream of the jump. In

Some additional intuition into the meaning of the dimensionless parameters can be gained by supposing temporarily that the fluid in the flume has uniform potential vorticity, a special case for which a theory exists (see Whitehead, et al., 1974; Gill, 1977). In particular, if $u_1(y)$ is geostrophically balanced, then the theory of Gill (1977) predicts the depth at section 1 to be

$$h_1(y) = h_0 - \Delta H_1 \sinh[(y - w_1/2)/L_d]/\sinh[w_1/2L_d] + (\bar{H}_1 - h_0)\cosh[(y - w_1/2)/L_d]/\cosh[w_1/2L_d] \quad (3.9)$$

where

$$\Delta H_1 = (h_{1-} - h_{1+})/2$$

and where

$$L_d = (gh_0)^{1/2}/f, \quad (3.10)$$

is the 'global' deformation radius based on the depth h_0 at which the relative vorticity ($\approx -u_y$) vanishes. This last condition holds in the laboratory reservoir within an error $-u_y/f < 0.3$, and h_0 will therefore be called the reservoir depth. According to (3.9), the flow is contained in boundary layers of width L_d along each side wall. The scale L_d also gives the decay scale for stationary Kelvin waves and is the decay scale of the jump in Fig. 1. This decay scale should be distinguished from the 'local' deformation radius $(g\bar{H}_1)^{1/2}/f$ which, according to (3.8) is related to the separated stream width. In the present experiment, h_0 is always larger than $\bar{H}_1$ by a factor of ten and hence L_d is always $\gg w_1$. This scale mismatch places the experimental parameter settings closer to those of Nof (1986) than those of Pratt (1983). In the limit $w_1/L_d \to 0$ (3.9) reduces to

$$h_1(y) = h_{1-} + (f^2 w_1/2g - 2\Delta H_1/w_1)y - f^2 y^2/2g. \quad (3.11)$$

To prevent additional parameters from becoming important, steps must be taken to insure that undesirable centrifugal and frictional effects do not influence the structure of the jump. Centrifugal acceleration acting over the along-channel length L of the jump will impart a force per unit density of magnitude $4f^2H_mRWL$, where R is the mean distance from the center of rotation and H_m is the mean depth through the jump. Also bottom friction acting over the interior of the jump imparts a force per unit density approximately equal to $c_dU_m^2LW$, where U_m is the mean velocity in the jump and c_d is a dimensionless drag coefficient having value 0.008 ± 0.002 for the painted flume bottom (Chow, 1959). These forces should be small compared to the typical momentum flux $U_m^2H_mW$ if friction and centrifugal acceleration are to be neglected. As discussed later, there is some ambiguity in defining L; however, if we choose W as a scale for L, as the experiments will indicate, then the ratio $R_c = 4f^2RW/U_m^2$ must be small to discount centrifugal effects and c_dW/H_m must be small to discount friction. Using the typical experimental values $f = 0.7\ s^{-1}$, $R \approx 10$ cm, $W = 20$ cm, $U_m \approx 50$ cm s^{-1}, and $H_m = 2$ cm gives $R_c \approx 0.2$ and $c_dW/H_m \approx 0.1$. Some high rotation cases were run in which R_c was not small, and these cases will be noted.

4. Experimental results

The qualitative effect of rotation in the experiments was found to be largely independent of Froude number $\bar{F}_1$. Figure 4 shows the evolution of the jump as rotation is increased when $\bar{F}_1$ initially has value 7.1. ($\bar{F}_1$ varies by no more than 0.5 between photographs.) The flow at the low rotation rate $r_1 = 0.22$ is shown in Fig. 4a. The fluid remains attached to both side walls and the jump is essentially no different in character than its nonrotating counterpart. The only hint of rotation is that a finite angle α exists between the line of depth discontinuity and the y-axis (as defined in Fig. 3a). Figure 4b shows the effect of increasing the rotation to the

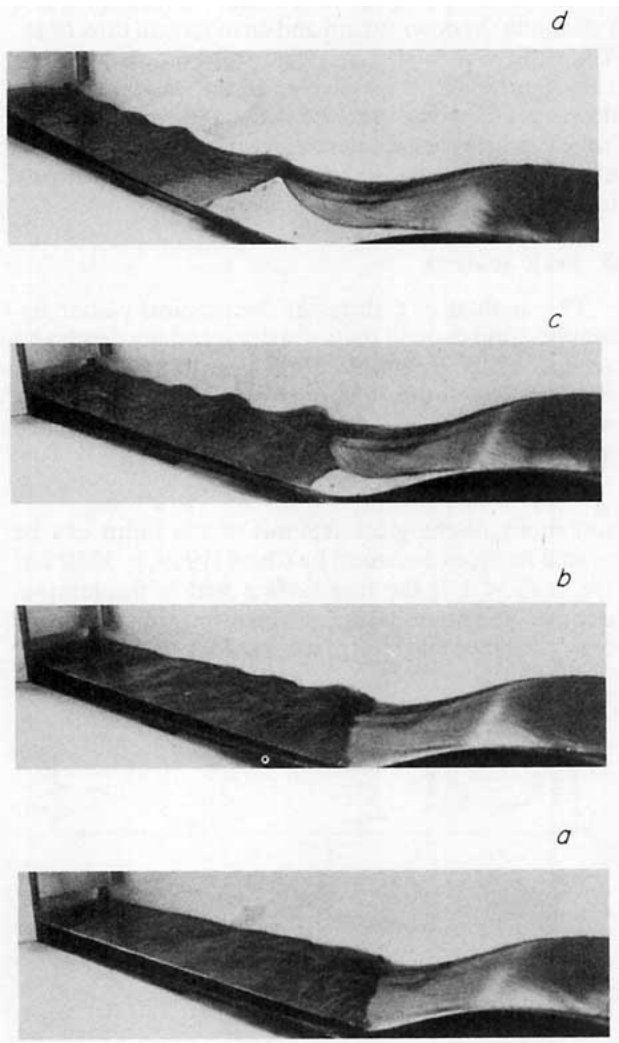

FIG. 4. Photographs of jump at various rotation rates. (a) $r_1 = 0.22$, $\bar{F}_1 = 7.1$; (b) $r_1 = 0.84$, $\bar{F}_1 = 6.6$; (c) $\hat{r}_1 = 3.1$, $\bar{F}_1 = 7.2$; (d) $\hat{r}_1 = 4.7$, $\bar{F}_1 = 7.6$.

point where separation of the supercritical flow is incipient ($\hat{r}_1 \approx 1.0$). The tendency of the fluid approaching the jump to be deflected to the right due to Coriolis acceleration is now more pronounced, and the angle α has increased. Also a train of stationary waves has begun to appear against the right wall in the lee of the jump. Despite these features, the sharp discontinuity in fluid depth that characterizes the nonrotating jump remains. In Fig. 4c the rotation has been increased to the point $\hat{r}_1 = 3.1$. The supercritical flow has separated from the left wall slightly downstream of the obstacle sill, but becomes reattached near the original position of the jump. The reattachment is abrupt and the stream width is practically discontinuous. On the right wall, signs of vertical-plane turbulence such as bubbles and small waves have begun to diminish. The line along which sudden depth change occurs resembles an oblique hydraulic jump and α has increased to a value $\approx 45°$. Also the stationary waves have grown in amplitude and extend several channel widths downstream and the total depth increase is distributed over this distance. Although some of this depth change is due to centrifugal effects, the greater part is due to the flow dynamics (as suggested by the scale arguments at the end of the previous section). Finally, Fig. 4d shows the flow at relatively high rotation ($\hat{r}_1 = 4.7$). The discontinuity is now completely one of width, rather than depth, and no visual signs of vertical plane turbulence are present. In this last case, centrifugal effects are large enough to invalidate the scaling arguments made previously. However, the photograph is shown to convince the reader that separation of the downstream part of the jump fails to occur even at extreme rotation rates.

Figure 5 shows a cross section of the separated supercritical flow slightly upstream of the jump for $\hat{r}_1 = 5.2$ and $\bar{F}_1 = 6.8$. The observed profile is indicated by the crosses, each of which represents a single measurement of the free-surface elevation using the point gauge. The deepest portion of the stream is concentrated along the right wall. To the left lies a thin, flat viscous region whose thickness is roughly the Ekman thickness $\delta_E = (2\nu/f)^{1/2}$ based on the kinematic viscosity ν of the fluid, as indicated by the dashed line. The depth of the viscous layer vanishes abruptly near the left wall. The stream is thus characterized by two widths, the first being the actual width and the second being the width of the inviscid portion of the stream near the right wall. Since most of the mass flux (in this case about 80 percent) is typically carried by the inviscid portion of the stream, the viscous layer is simply ignored and w_1 is taken as the inviscid width. In most cases the inviscid portion of the stream can easily be distinguished by the naked eye and w_1 can be determined unambiguously. The solid curve in Fig. 5 is the theoretical, 'zero' potential vorticity (i.e., $w_1/L_d \to 0$) profile computed from (3.11) with the observed values of f, Q and w_1. Agreement between the observed and theoretical profiles is fairly reasonable indicating that the potential vorticity of the fluid in inviscid portion of the stream is fairly low and uniform. The irregularity of the observed profile is due to the presence of small stationary cross-waves (which appear in most laboratory supercritical flows).

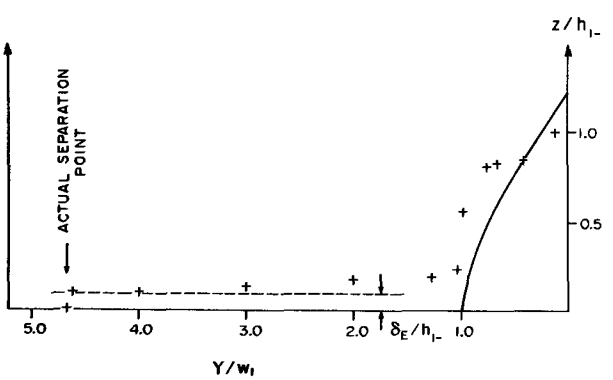

FIG. 5. Observed (+++) and theoretical (———) depth profiles for the case $\bar{F}_1 = 6.8$, $\hat{r}_1 = 5.2$. The dashed line shows the dimensionless Ekman height $\delta_E/h_{1-} = (2\nu/fh_{1-}^2)^{1/2}$. The observed dimensional quantities used to obtain the theoretical profile are $Q = 0.36\ \mathrm{L^3\ s^{-1}}$, $f = 1.98\ \mathrm{s^{-1}}$, $w = 3.0$ cm. The dimensional wall depth is 1.1 cm.

Figure 6 shows the extent of the parameter space r_1 (or $\hat{r}_1$), $\bar{F}_1$ in which stationary shocks were found in the experiment. Above the dashed line $\bar{F}_1 = 2/r_1$ the upstream flow is separated. Jumps in which stationary waves are observed are indicated by dots, those without by triangles. Also the angle α formed between the line of abrupt depth change and the y-axis is indicated next to each dot. The general tendency is for α to increase with increasing $\bar{F}_1$ and $\hat{r}_1$. The absence of an α value next to a dot indicates that no line of abrupt change is observed, as is generally the case for $\hat{r}_1 > 4.0$. The α-values represent cross-channel averages only. Pratt (1983) has shown that any discontinuity in fluid depth at a wall must occur along a line perpendicular to the wall. This property does appear to be a feature of the shocks in Fig. 4; however, the line is clearly oblique to the walls in the interior.

Figure 7 shows a fairly representative map of the horizontal velocity structure near the jump. The inviscid portion of the supercritical flow is separated here ($\hat{r}_1 = 2.5$); however a thin, viscous region also exists (as in Fig. 5) making contact with the left wall and giving the appearance of nonseparation. Downstream of the point of reattachment the flow is concentrated in a jet which flows along the right wall. Estimates of the horizontal surface velocity obtained from streak photographs appear in Fig. 7 along with corresponding values of the local Froude number $F = u(x, y)/[gh(x, y)]^{1/2}$. It is well known (Chow, 1959) that the requirement for stationary cross waves to exist locally in the flow is that $F > 1$, and it can be seen that this requirement is satisfied along the right wall. The suggestion, then, is that the stationary waves shown in Figs. 46b–

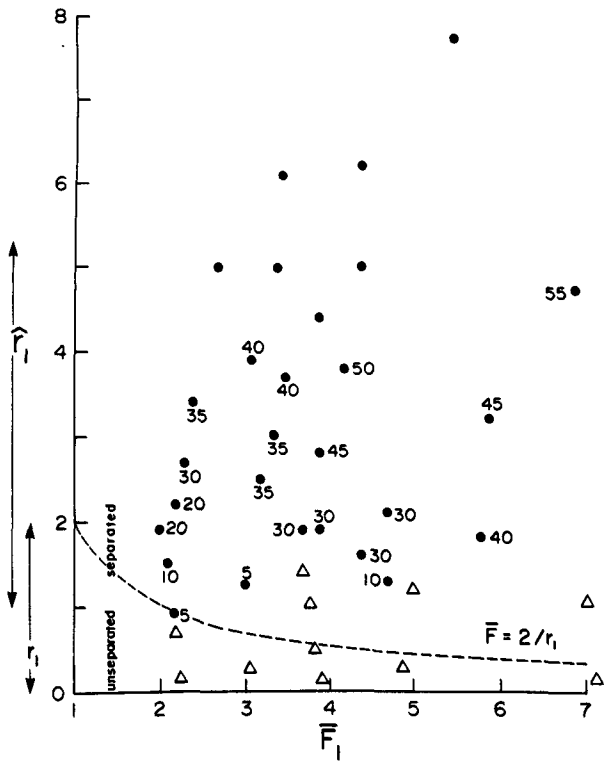

FIG. 6. Location of stationary waves in terms of Froude number $\bar{F}_1$ and Burger number r_1 (or $\hat{r}_1$). Dots represent flow with stationary waves and triangles represent flow without stationary waves. The angle of obliquity α is indicated in degrees where appropriate. The upstream flow is separated above the dashed line and there $\hat{r}_1$ should be used as the abscissa.

c are cross waves lying in a 'locally supercritical' region. Along the left wall the flow is dominated by time-dependent eddy motions, with typical velocities an order of magnitude less than those along the right wall. As one moves downstream, the right wall velocities diminish and the mass flux becomes more evenly distributed across the channel width. This picture holds for $r_1 \geq 0.2$ and remains qualitatively unchanged even after separation occurs upstream of the jump.

5. Theory

How do long waves fit into the picture described above? First consider the propagation of long waves in the separated flow. Since $w/L_d \ll 1$, the results of Stern (1980) would appear to be the most relevant and he shows that two long-wave modes exist. The dynamics of the first are essentially those of a Kelvin wave and this mode always propagates downstream. The second mode is associated with the free (left hand) edge of the current and propagates in the direction of the right-hand wall velocity. Since the latter is observed to be positive in all cases, the frontal mode also propagates downstream and the flow is therefore unambiguously supercritical. These properties also apply to separated flows with 'finite' potential vorticity (i.e., $w/L_d = 0(1)$). In particular, the frontal wave always propagates in the direction of the wall velocity (see Kubokawa and Hanawa, 1984a).

Turning now to the downstream (unseparated) portion of the flow one may use the results of Gill (1977) or Pratt (1983). Both authors show that the two long-wave modes are Kelvin waves, each trapped against a separate wall. The wave associated with the left wall can propagate upstream provided that $\bar{U} < (g\bar{H})^{1/2}[1 - T^2(1 - \bar{H}/h_0)]^{1/2}$ where $T = \tanh(w/2L_d)$ (cf. Eq. 3.19 in Pratt, 1983). When $w/L_d \ll 1$, this requirement reduces to $\bar{U} < (g\bar{H})^{1/2}$ or $\bar{F} < 1$, as observed in the experiment. Hence the nonseparated flow downstream of the region of abrupt width change is apparently subcritical.

Nof's (1984) calculations show that stationary shocks cannot exist when the entire flow is separated. This result can be interpreted as meaning that the frontal wave dynamics cannot support stationary shocks.

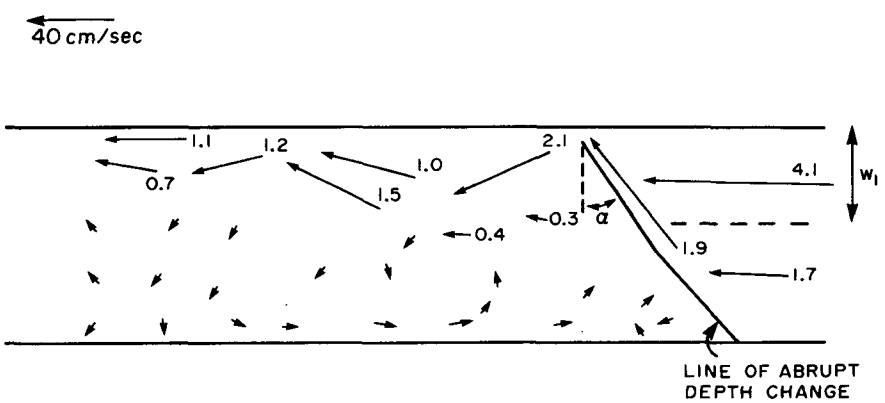

FIG. 7. Horizontal circulation for case $\hat{r}_1 = 2.5$, $\bar{F}_1 = 6.0$ as deduced from streak photographs. Note that the actual stream width is equal to the channel width W upstream, whereas the inviscid width w_1 (dashed line) is $< W$. The downstream edge of the obstacle lies approximately where the line of abrupt depth change begins.

On the other hand, suppose that the downstream portion of the shock is attached, allowing the left-wall Kelvin wave to come into play. Does shock-joining theory then allow stationary shocks? Nof's calculation can easily be repeated for the new case and the answer is yes. The procedure is to specify values of $\hat{r}_1$ and $\bar{F}_1$ describing a separated, supercritical flow and search for a conjugate attached state $(r_2, \bar{F}_2)$ having the same flow rate, flow force and potential vorticity.

The statements of flow rate and flow force conservation are

$$\bar{h}_1 \Delta h_1 = \bar{h}_2 \Delta h_2 \tag{5.1}$$

$$\int_0^{w_1} (h_1 u_1^2 - f\psi_1 + g h_1^2/2)dy = \int_0^{W} (h_2 u_2^2 - f\psi_2 + g h_2^2/2)dy \tag{5.2}$$

which follow directly from Nof's (1984) Eqs. (3.7) and (3.14). The streamfunction ψ_n is defined by $\partial\psi_n/\partial y = -u_n h_n$ and $\partial\psi_n/\partial x = v_n h_n$, and it follows from the geostrophic relation for u_n that

$$\psi_n = (g/2f)[h_n^2(y) - h_{n-}^2] \quad (n = 1 \text{ or } 2),$$

where the value of ψ_n has been chosen as zero at the right wall. Substituting this expression into (5.2) gives

$$\int_0^{w_1} h_1 u_1^2 dy + g h_{1-}^2/2 = \int_0^{W} h_2 u_2^2 dy + g h_{2-}^2/2. \tag{5.3}$$

The depth profiles, obtained using the appropriate width w_1 or W in (3.11) can be written

$$h_1(y) = \bar{H}_1[-2\bar{F}_1^{-2}(y/w_1)^2 + 2(\bar{F}_1^{-2} - 1)y/w_1 + 2] \tag{5.4}$$

$$h_2(y) = \bar{H}_2\left[-\frac{1}{2}r_2^2(y/W)^2 + \left(\frac{1}{2}r_2^2 - r_2\bar{F}_2\right)(y/W) + \left(1 + \frac{1}{2}r_2\bar{F}_2\right)\right]. \tag{5.5}$$

The geostrophic velocity profiles are thus

$$u_1(y) = \bar{U}_1[2\bar{F}_1^{-2}(y/w_1) - (\bar{F}_1^{-2} - 1)] \tag{5.6}$$

$$u_2(y) = \bar{U}_2\left[\bar{F}_2^{-1}r_2(y/W) - \left(\frac{1}{2}\bar{F}_2^{-1}r_2 - 1\right)\right]. \tag{5.7}$$

Substituting for u_1, h_1, u_2, and h_2 in (5.1) and (5.3) and nondimensionalizing the results, one obtains

$$8\bar{F}_2\hat{r}_1^4 = r_2^3\bar{F}_1^4 \tag{5.8}$$

$$(\bar{F}_1^6/16\hat{r}_1^5)\{-16/10\bar{F}_1^6 + 8/3\bar{F}_1^4 + (\bar{F}_1^{-2} - 1)[4/\bar{F}_1^4 - 4/\bar{F}_1^2 + 3(\bar{F}_1^2 - 1)^2 - 10(\bar{F}_1^{-2} - 1)/\bar{F}_1^2] + 2/\bar{F}_1^2\}$$
$$= r_2^{-4}\left\{\left(-r_2^4/10 + \frac{1}{2}r_2^3\left(\frac{1}{2}r_2 - \bar{F}_2\right) + \frac{1}{2}\left[\left(\frac{1}{2}r_2 - \bar{F}_2\right)^3 r_2 - 2r_2\left(\frac{1}{2}r_2 - \bar{F}_2\right)\left(1 + \frac{1}{2}r_2\bar{F}_2\right)\right]\right.$$
$$\left. + \frac{1}{6}\left[2r_2^2\left(1 + \frac{1}{2}r_2\bar{F}_2\right) - 5r_2^2\left(\frac{1}{2}r_2 - \bar{F}_2\right)^2\right] + \left(\frac{1}{2}r_2 - \bar{F}_2\right)^2\left(1 + \frac{1}{2}\bar{F}_2 r_2\right)\right\} + \left[\left(1 + \frac{1}{2}r_2\bar{F}_2\right)^2 \Big/ 2r_2^4\right]. \tag{5.9}$$

By eliminating r_2 between these two equations it is possible to form a fourth-order polynomial for $\bar{F}_2^{2/3}$ whose coefficients depend upon $\hat{r}_1$ and $\bar{F}_1$. For practical purposes, however, it is easier to solve (5.8) and (5.9) in present form using a method due to Powell (1970) and the results of this calculation are shown in Fig. 8. Stationary shocks are possible only for values of $\hat{r}_1$ and $\bar{F}_1$ lying to the right of the contour $\bar{F}_2 = 1$. To the left of this line no physically meaningful roots of (5.8) and (5.9) exist. To the right can be found a family of subcritical downstream states whose Froude number decreases as the upstream Froude number increases, also a property of nonrotating jumps. It has been verified that the fluid passing through the shocks experiences an energy loss. The experimental values of $\bar{F}_1$ and $\hat{r}_1$ for which stationary shocks are found (indicated by dots in Fig. 8) lie, for the most part, to the right of the contour $\bar{F}_2 = 1$. The only exceptions lie fairly close to the $\bar{F}_2 = 1$ contour and the discrepancies could easily be due to measurement error or to sources of momentum or potential vorticity within the jump.

Although the theory and experiment agree fairly well as to the conditions under which stationary shocks can occur, detailed comparisons between the predicted and observed downstream states are less successful. For example, consider the shock which occurs when $\hat{r}_1 = 4.0$ and $\bar{F}_1 = 3.25$ which, according to Fig. 8 and Eq. (5.8) has the downstream values $r_2 = 2.33$ and $\bar{F}_2 = 0.69$. The downstream velocity profile is thus given by (5.7) as

$$u_2(y) = \bar{U}_2[3.38(y/W) - 0.69].$$

This profile indicates a reverse flow $u_2 < 0$ along the right wall, whereas the observations seem to indicate that $u_2 > 0$ along the right wall in all cases (for example, Fig. 7). One explanation for this discrepancy, as discussed in the next section, is that the rotating tank is too short to allow the downstream conjugate state to develop fully.

6. Discussion

The experiments show that flow separation from the sidewall leads to a shock structure drastically different from that of the nonseparated solutions obtained by Pratt (1983) and Nof (1986). The most obvious differ-

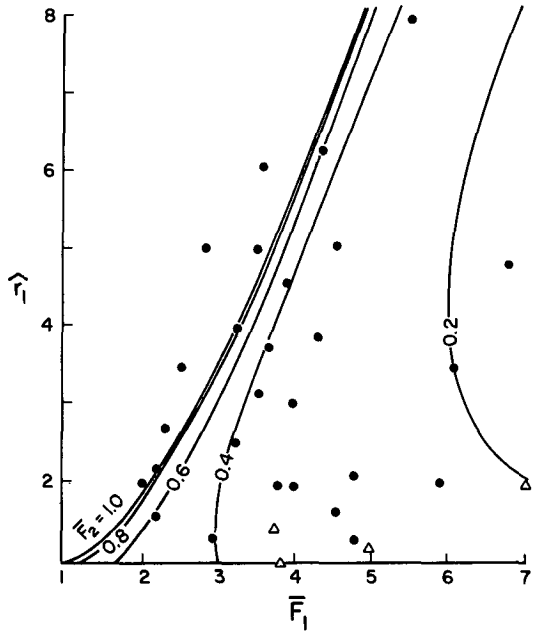

FIG. 8. Downstream Froude number $\bar{F}_2$ as function of $\bar{F}_1$ and $\hat{r}_1$ for stationary shocks in which flow is separated upstream and attached downstream.

ence is that the latter are characterized by sudden changes in fluid depth, while the former are characterized by sudden changes in stream width with gradual, wavelike changes in depth. One consequence is that the turbulence in the separated shock is associated with horizontal eddies (see Fig. 7) having length scales much larger than the fluid depth whereas sudden depth changes tend to produce vertical-plane eddies which scale with the fluid depth (Bakhmeteff and Matzke, 1936). It is not uncommon for deep outflows to widen rapidly while exiting straits, one example being the deep outflow from the Jungfern Passage. Sturges (1975, Figs. 4 and 5) observed this current to widen and thicken appreciably downstream of the sill and to entrain upper fluid in the process. These features may indicate a shock, possibly of the type shown here, but may also be due to some other mechanism such as topographic steering or bottom friction.

What would happen to the shock if the downstream end wall was moved to $x = -\infty$, as would better typify the oceanic prototype? It is wrong to suppose that the shock would disappear; even without the end wall a shock would be triggered by the weak force due to bottom friction. With no rotation, it is known that the shock would then take the form of an undular hydraulic jump (Chow, 1959). Presumably, the rotation of this jump would lead to the same sorts of qualitative effects observed here.

One matter which remains unsettled is the definition of the shock length, that is, the along-channel distance over which the shock occurs. In the nonrotating case the shock is *defined* to include the region in which the sudden depth change occurs in addition to the region in which major turbulent features and lee waves exist (see Chow, 1959, for more details). Accordingly, one might define the shocks of Figs. 4c, d to begin at the point of reattachment and to include all cross waves and major turbulent features in the lee. Visual evidence then suggests that the jump extends at least several channel widths downstream of the point of reattachment and probably runs into the end wall at higher $\hat{r}_1$ values. This conclusion is supported by the inability of the shock-joining theory to predict the velocity structure of the downstream end state. To insure that the upstream portion of the shock was not sensitive to the end conditions, these conditions were altered in a variety of ways (the withdrawal tubes were rearranged and different types of submerged obstacles were placed in the flow path at the end of the tank); none were found to change the qualitative structure near the region of abrupt width change.

There is clearly a need for a more sophisticated and refined version of the crude experiment described here. The use of a longer tank might allow the downstream end state of the shock to become fully developed. Also, detailed velocity and depth measurements of the end states would provide information concerning the conservation of potential vorticity and implications for shock-joining theory. Unfortunately, such an experiment would require a larger turntable than the 2-meter diameter table used here and considerable contamination from centrifugal accelerations might occur. Experiments using two immiscible fluids could overcome this difficulty since the deformation radius L_d would be reduced in proportion to the square root of the density difference. However, the parameter w_1/L_d would no longer be small and the experimental results would depend upon three (rather than two) dimensionless parameters. A cleaner approach to the problem might be made numerically, provided that numerical methods can be developed which are able to handle both flow separation and abrupt depth changes.

Acknowledgments. This work was supported partially by the Office of Naval Research under Contract N00014-81-C-0062 and partially by the National Science Foundation under Grant OCE85-15655. The author would like to thank Dr. John Whitehead and Mr. Robert Frazel for help in the laboratory, Ms. Barbara Gaffron for help in preparing the manuscript, and the reviewers for their valuable comments.

REFERENCES

Bakhmeteff, B. A., and A. E. Matzke, 1936: The hydraulic jump in terms of dynamic similarity. *Trans., Amer. Soc. Civil Eng.*, **101**, 630–647.

Chow, V. T., 1959: *Open-Channel Hydraulics*, McGraw-Hill, 680 pp.

Gill, A. E., 1977: The hydraulics of rotating-channel flow. *J. Fluid Mech.*, **80,** 641–671.

Houghton, D. D., 1969: Effect of rotation on the formation of hydraulic jumps. *J. Geophys. Res.*, **74,** 1351–1360.

Kubokawa, A., and K. Hanawa, 1984a: A theory of semigeostrophic gravity waves and its application to the intrusion of a density current along a coast. Part I. Semigeostrophic gravity waves. *J. Oceanogr. Soc. Japan,* **40,** 247–259.

——, and ——, 1984b: A theory of semigeostrophic gravity waves and its application to the intrusion of a density current along a coast. Part II. Intrusion of a density current along a coast in a rotating fluid. *J. Oceanogr. Soc. Japan,* **40,** 260–270.

Nof, D., 1984: Shock waves in currents and outflows. *J. Phys. Oceanogr.*, **14,** 1683–1702.

——, 1986: Geostrophic shock waves. *J. Phys. Oceanogr.*, in press.

Powell, M. J. D., 1970: A hybrid method for nonlinear equations. *Numerical Methods for Nonlinear Equations,* P. Rabinowitz, Ed., Gordon and Breach, 482 pp.

Pratt, L. J., 1983: On inertial flow over topography, Part 1. Semigeostrophic adjustment to an obstacle. *J. Fluid Mech.*, **131,** 195–218.

Stern, M. E., 1980: Geostrophic fronts, bores, breaking and blocking waves. *J. Fluid Mech.*, **99,** 687–703.

Sturges, W., 1975: Mixing of renewal water flowing into the Caribbean Sea. *J. Mar. Res.*, **33**(Suppl), 117–130.

Whitehead, J. A., 1985: A laboratory study of gyres and uplift near the Strait of Gibraltar. *J. Geophys. Res.*, **90**(C4), 7045–7060.

——, A Leetmaa and R. A. Knox, 1974: Rotating hydraulics of strait and sill flow. *Geophys. Fluid Dyn.*, **6,** 101–125.

Williams, R. T., and A. M. Hori, 1970: Formation of hydraulic jumps in a rotating system. *J. Geophys. Res.*, **75,** 2813–2821.

Yih, C. S., H. E. Gascoigne and W. R. Debler, 1964: Hydraulic jump in a rotating fluid. *Phys. Fluids,* **7,** 638–642.